Journal of Enzyme Inhibition and Medicinal Chemistry, April 2005; 20(2): 129–134

Molecular mechanics PBSA ligand binding energy and interaction of Efavirenz derivatives with HIV-1 reverse transcriptase

PHILIPP WEINZINGER[1], SUPA HANNONGBUA[2] & PETER WOLSCHANN[1]

[1]*Institute for Theoretical Chemistry and Structural Biology, University of Vienna, Waehringer Strasse 17, Vienna 1090, Austria, and* [2]*Department of Chemistry, Faculty of Science, Kasetsart University, Bangkok 10900, Thailand*

(Received 26 June 2004; accepted 4 October 2004)

Abstract

In order to evaluate the properties of several HIV-1 reverse transcripase(RT) inhibitors, Efavirenz (SUSTIVA®) and a set of its derivatives (benzoxazinones) have been placed into the nonnucleoside analogue binding site of the enzyme by molecular docking. The resulting geometries were used for a molecular dynamics simulation and binding energy calculations. The enzyme-inhibitor binding energies were estimated from experimental inhibitory activities (IC_{90}). The correlation of the predicted and experimental binding energies were satisfactory acceptable as indicated by $r^2 = 0.865$. Based on MD simulations, the obtained results indicate that the tight association of the ligand to the HIV-1 RT binding pocket was based on hydrogen bonding between Efavirenz's N1 and the oxygen of the backbone of Lys 101, with an estimated average distance of 1.88 Å. Moreover, electrostatic interaction was mainly contributed by two amino acid residues in the binding site; Lys 101 and His 235. MD simulations open the possibility to study the reaction of the flexible enzyme to those substances as well as the overall affinity.

Keywords: *HIV-1 reverse transcriptase, Efavirenz, molecular dynamics, ligand binding energy, MM-PBSA, inhibition*

Introduction

The HIV-1 reverse transcriptase (RT) is a major target for many anti-AIDS drugs. A distinction of the functionality of its inhibitors splits them into two groups: the nucleoside reverse transcriptase inhibitors (NRTIs) and the non-nucleoside RT inhibitors (NNRTIs). The NRTIs bind to the active site instead of a dNTP and cause termination of the growing DNA. They can also be incorporated by the host DNA polymerases and, therefore, cause serious side effects, especially damage to the mitochondria. NNRTIs on the other hand bind allosteric to the unique binding site 10 Å apart form the active site [1] although they are chemically and structurally diverse. This uniqueness of NNRTIs leads to the high specificity and low cytotoxicity of this group of anti-HIV agents. However, all currently FDA approved NNRTIs suffer from the evasion of the enzyme by drug resistance mutations. Efavirenz [2] ((4*S*)-6-chloro-4-(cyclopropylethynyl)-4-(trifluoromethyl)-1,4-dihydro-2H-3,1-benzoxazin-2-one) as a second-generation inhibitor fares better but still is rendered ineffective by most common mutations [3,4]. As a consequence, the search for new NNRTIs is an ongoing endeavour and any leads to the understanding of worthwhile inhibitor properties and the mechanism of inhibition are still sought after.

The HIV RT enzyme itself is a heterodimer containing two separate chains with identical amino acid sequences, but of different length, p66 and p51 (Figure 1) according to their molecular weight [5]. Due to its appearance in p66, distinct domains have been named fingers (residues 1–84, 120–150), palm (85–119, 151–243), thumb (244–322), connection domain (323–437) for both p66 and p51. p66 harbours an additional RNase H domain (438–560).

The DNA polymerase is located on the p66 chain with its catalytic centre on the fingers subdomain.

Correspondence: P. Weinzinger, Institute for Theoretical Chemistry and Structural Biology, University of Vienna, Waehringer Strasse 17, Vienna 1090, Austria. Tel: 43 1 4277 52774. Fax: 43 1 4277 9527. E-mail: philipp.weinzinger@tbi.univie.ac.at

ISSN 1475-6366 print/ISSN 1475-6374 online © 2005 Taylor & Francis Ltd
DOI: 10.1080/14756360400020520

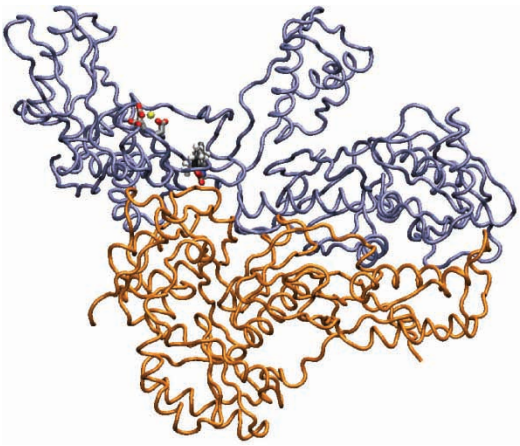

Figure 1. HIV-1 RT in the open inhibited conformation showing p66 (blue), p51 (orange), the catalytic Asp triad with a Magnesium ion (yellow) and the inhibitor Efavirenz in the groove between the fingers (the left branch) and the thumb domain (middle) of p66. The right branch of p66 is the RNase H domain.

The thumb domain is the most flexible [6]. It can rotate at a hinge region next to the palm domain and close the gap to the fingers domain. This is called the closed hand conformation, which is predominantly adopted by the ligand free enzyme [7]. If DNA is present, RT opens its hand and the DNA chain is placed between the fingers and the thumb domains. A bound NNRTI prevents the protein from closing. The details of the mechanism for this process is still in debate.

Major subdomain rearrangements in HIV-1 Reverse Transcriptase upon DNA binding were studied by Molecular Dynamics (MD) simulations [5,8]. Prior studies [9] aimed at collecting of various descriptors derived from Monte Carlo simulations. Those included the Lennard–Jones contribution and a hydrophobic surface terms in the case of Efavirenz derivatives. Other works [10] concentrated on specific mutations using free energy perturbation methods [11]. However, a detailed analysis of the flexibility of the HIV-1 RT complexed with Efavirenz has not been reported yet. Therefore, the objectives of this work are to investigate the flexibility of Efavirenz and its derivatives complexed with HIV-1 RT and to observe the main interaction of the inhibitors with the particular amino acid residues in the HIV-1 RT binding site during a MD simulation. This fundamental structural information will be helpful for the understanding of the enzyme-inhibitor interaction, especially, for the design of new more potent inhibitors active against mutant HIV-1 RT.

Methods

The X-ray structure of Efavirenz bound to HIV-1 [12] (PDB entry 1fk9) was selected as starting structure for the docking calculations and the subsequent molecular dynamics simulations. The missing residues were reconstructed with the help of other X-ray structures (PDB code 1fko, 1jkh) and subsequent low temperature annealing and energy minimization procedures of the added residues while constraining the known X-ray residue positions. A set of RT inhibitors and their experimental IC_{90} values were taken from the literature [13,14]. RESP (restrained electrostatic potential) charges [15,16] were calculated with the *Gaussian 03* program [17] using the HF/6-31G$^{(d)}$ basis set. The 13 Efavirenz derivatives (Table I) were docked into the binding pocket using *FlexX* [18]. All ligands showed a similar binding mode compared to the Efavirenz crystal structure with the exception of compound H, which it was not possible to dock into the binding site at all. This compound was placed manually in a comparable mode. A water cap with a radius of 30 Å and consisting of 1685 water molecules was added with its centre located at the NNRTI binding site (Figure 2). The *AMBER7.0* program package [19] was used for the molecular dynamics simulation. During the MD simulations only residues within 15 Å of the inhibitor

Table I. HIV-1 RT inhibitory activity and experimental binding free energy calculated from IC_{90} values of benzoxazinones. All compounds were assayed for whole cell based antiviral activity. The IC_{90} values were determined for racemic mixtures, except compound A, which is Efavirenz itself. Those values have been halved for the calculation of the free binding energy since only the *S*-enantiomer is active. The following approximation was used for the calculation: $\Delta G_{binding} \approx RT \ln(\text{activity})$. This estimate contains errors, which lie in an acceptable range for this data set. The exact binding energy of Efavirenz [2] (cmpd. A) is −11.713 kcal/mol derived from the K_i value of 2.93 nM.

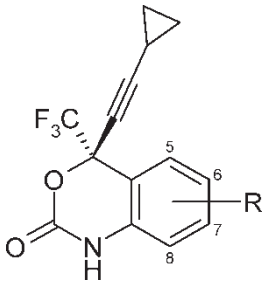

Cmpd.	R	IC_{90} (nM)	experimental ΔG (kcal/mol)
A	6-Cl	2.03	−11.93
B	H	10.31	−11.38
C	6-F	7.35	−11.58
D	6-iPr	27.84	−10.78
E	6-OCF_3	18.89	−11.02
F	5-F, 6-F	3.15	−12.08
G	5-F, 6-F, 8-F	14.02	−11.05
H	6-Cl, 8-OCH_3	122	−9.9
I	6-OCH_3	2	−12.35
J	5-F	4.34	−11.89
K	6-NO_2	0.83	−12.88
L	6-NH_2	20.59	−10.96
M	6-N(H)CH_3	9.02	−11.46

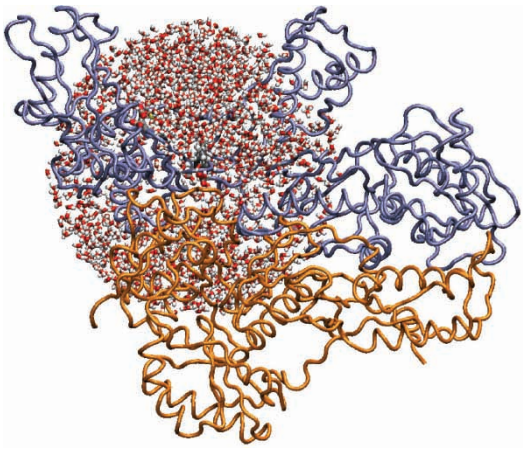

Figure 2. HIV RT with the water shell centred at the location of the inhibitor Efavirenz. Only residues within the sphere were mobile during the MD simulations.

(residues 91–110, 172–202, 222–240, 316–321, B135–B141), the water molecules and the ligands were allowed to move. The MD simulation was performed for 500 ps at 300 K with the Berendsen temperature-coupling algorithm [20] using the parm99 force field for the protein and the general amber force field for the ligands. Bonded and non-bonded interactions between moving and frozen atoms were treated identically. These restrained simulations have the advantage of a fast equilibrating system [21]. Following the systems equilibration after 100ps, the subsequent 400 ps of the generated trajectory were used to extract 100 snapshots for further analysis.

The MM-PBSA (Molecular Mechanics—Poisson-Boltzmann/Surface Area) methodology [21,22] allows the calculation of the complete binding reaction energy including the desolvation of the ligand and the unbound protein. A full thermodynamic cycle is given in Figure 3. The Lennard–Jones and electrostatic interactions were calculated using *AMBER* analysis tools. In addition, estimates of the entropic contribution TΔS is available using the *nmode* module of *AMBER*. Only 15 snapshots were used for this lengthy procedure. The desolvation energies can be approximated using continuum solvent approaches. The VdW (Van der Waals) contribution of the desolvation process is available through the surface area [23] calculated by the *molsurf* program employing

$$\begin{array}{ccccc} RT_{aqu} & + & Lig_{aqu} & \xrightarrow{\Delta G_{binding}} & RT/Lig_{aqu} \\ \downarrow -\Delta G^{RT}_{solv} & & \downarrow -\Delta G^{Lig}_{solv} & & \downarrow -\Delta G^{RT/Lig}_{solv} \\ RT_{gas} & + & Lig_{gas} & \xrightarrow{\Delta G_{gas}} & RT/Lig_{gas} \end{array}$$

Figure 3. Thermodynamic cycle of a ligand binding process. ΔG_{gas} is available through the interaction between protein and ligand (ΔH_{gas}) and TΔS. The three ΔG_{solv} are estimated with the help of the Poisson–Boltzmann equation and a surface area term.

an algorithm developed by Conolly [24]. The Poisson–Boltzmann equation gives the electrostatic energy to the solvent. *APBS* [25] (Adaptive Poisson–Boltzmann Solver) was used for this calculation. Again, since this is a very time consuming procedure not all 100 snapshots were subject to this procedure.

Strictly, the MM-PBSA method allows an exact calculation of $\Delta G_{binding}$ only if no conformational changes occur in the protein during the binding process because all parameters are derived from one MD simulation. Nevertheless this is not true for HIV-1, because the binding pocket does not exist in the unliganded enzyme. It is only created through partially large movements of the side chains during the formation of the binding pocket (especially Tyrosine 188 [26]) in the process of ligand binding. Furthermore, a shift of the equilibrium between the open and closed hand conformation [7] occurs in favour of the open handed RT structure. However, the ranking of similar inhibitors is possible due to cancellation of errors of analogous motions. In order to correlate the calculated energy contribution to the experimental energies an approach similar to the linear response (LR) theory [27] is used. Here, ΔG is described by weighted VdW and Coulomb energies. The weights were determined by fitting the simulation results to known experimental values. This method was later expanded to include hydration energies [28].

Results and discussion

One of the main distinctive characteristics of the HIV-1 RT binding pocket is its flexibility. Small drugs like Efavirenz (30 atoms) and large inhibitors like Delavirdine [29] (60 atoms) bind to the enclosed hydrophobic pocket alike. With MD simulations, it is possible to characterize the effects the ligands have on the pocket, which helps to discern the interactions necessary for a tight association of the ligand. Beside the overall lipophilicity, the most important interaction with Efavirenz and most of its derivatives is hydrogen bonding to Lys 101. In the average structure obtained from MD simulations, Efavirenz's NH forms a H-bond with the Lys 101 backbone oxygen; $d_{HO} = 1.88$ Å, $\alpha_{NHO} = 166°$(Figure 4). Those values represent the state further away from the minimum caused by kinetics. For comparison in the X-ray structure, the H–N distance is 1.58Å with an angle of 154°. Another, weaker H-bond is formed by Efavirenz's carboxy O_2 and the backbone NH of Lys 101 ($d_{OH} = 2.13$ Å, $\alpha_{NHO} = 157°$ MD average; $d_{OH} = 2.02$ Å, $\alpha_{NHO} = 157°$ X-ray).

Hydrogen-bonding is a major contributor to the electrostatic interaction. Other Coulombic interactions are decompositioned into parts of +0.3 to −0.6 kcal/mol per residue of the hydrophobic pocket. Lys 101 and His 235 are an exception in this. Beside the hydrogen bond to Lys 101 two compounds, L and M, can form a hydrogen bond to the backbone oxygen of His 235 with

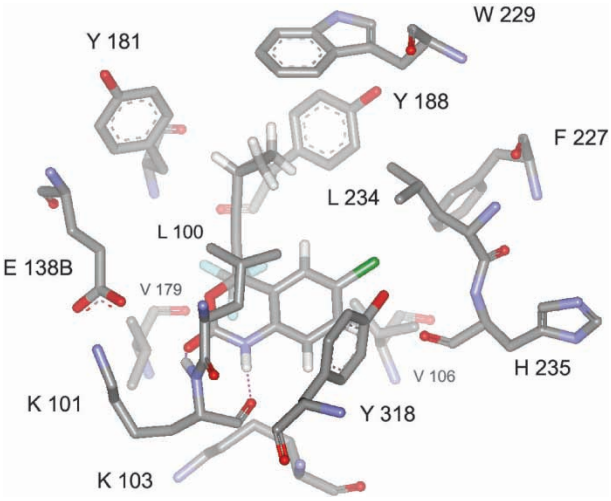

Figure 4. This structure of Efavirenz in the HIV-1 RT binding pocket was calculated by using the average positions during a MD simulation. The H-bonds to Lys 101 are displayed in dotted lines.

their amine group (Table II). Another exception is the Glutamate 138 of the B chain, which has a repulsive interaction primarily to the carboxylic O of all selected benzoxazinones. Since this group is common to all compounds no large deviations were found in the set. This repulsion is in the range of 2.2 ± 0.6 kcal/mol to the sum of hydrophobic and electrostatic energy contributions. Compound M gets an especially high penalty here since it is pushed towards Glu 138B in order to optimise the H-bond to His 235. Its interaction energy is 3.25 kcal/mol. The sidechain of Glu 138B is relatively rigid in its position since it forms a H-bond to the sidechain of Lys 101. It should be noted that a water molecule forms H-bonds to both Glu 138B and the exposed carboxylic oxygen of the Efavirenz derivatives during the whole simulation. The position of the water molecule between its hydrogen bonding partners is not optimal since it cannot completely prevent the repulsions of Glu 138B and the inhibitors. The positions of the three oxygens involved are best described as an isosceles triangle.

Table II. Interaction of certain RT residues with the bound ligand. Lys 101 and His 235 are the only residues with major electrostatic contributions to the overall electrostatic interaction to the binding pocket.

	Electrostatic contr.		Hydrophobic contribution		
Cmpd.	Lys 101	His 235	Tyr 181	Tyr 188	Tyr 318
A	−16.56	−1.52	−2.32	−5.51	−2.32
B	−13.97	−1.66	−2.64	−3.11	−1.91
C	−15.48	−1.57	−3.24	−3.95	−2.21
D	−11.41	−1.62	−2.5	−4.46	−2.11
E	−12.53	−1.14	−2.11	−3.02	−2.57
F	−14.94	−2.24	−3.31	−4.11	−1.93
G	−12.1	−2.14	−2.95	−3.82	−2.85
H	−10.48	−1.85	−3.02	−5.08	−4.13
I	−14.85	−0.95	−3.76	−4.02	−2.28
J	−14.96	−1.79	−3.29	−4.01	−1.91
K	−14.36	−1.67	−2.21	−5.17	−2.33
L	−14.69	−6.37	−3.11	−3.67	−2.58
M	−15.42	−7.88	−3.84	−4.66	−1.91
Avg.	−13.16	−2.49	−2.7	−3.92	−2.39

From all Van der Waals interactions the most important one is established between Leu 100 and the inhibitors. This residue is placed above the two-ring system of the benzoxazinones and can interact with the cyclopropylethynyl group. This is common for all compounds under study with only small deviations. The average potential is -5.74 ± 0.33 kcal/mol. A mutation to isoleucine at this position (L100I) is known to mediate resistance to Efavirenz. Another strong contact can be found to Tyr 188. Interaction with the cylopropyl group but also the alkyne group and to a smaller amount with the CF_3 group contributes to this value. Here Efavirenz (compound A) has the strongest interaction, which might explain its susceptibility to mutations at this residue. Another residue that shows a relatively large diversity among the selected compounds is Tyr 318. Compound H with its methoxy group has an outstanding affinity to this residue. In the vicinity of this group the x-ray structure is very tightly packed and the starting structure presented almost no space for this group. The good overall VdW interaction of this compound during the MD simulation and especially to the Tyr 318 can be credited to the flexibility of the binding pocket. Due to steric hindrance and the proximity of the NH group of the ligands, other interactions, especially H-bonding to Lys 101, are severely weakened. It is possible that the L100I mutation hampers this interaction for all compounds since the earlier branching of isoleucine clashes with Tyr 318.

Other high VdW interactions can be found all over the binding pocket for all ligands as a result of the flexibility of this binding pocket. The important ones with interactions greater than 1 kcal/mol are: Pro95: -1.29 ± 0.14 kcal/mol, Lys101: -1.99 ± 0.50 in addition to the hydrogen bonding, Lys 103: -2.68 ± 0.28, Val 106: -2.37 ± 0.34, Val 108: -2.50 ± 0.22, Trp 229: -1.74 ± 0.25, Leu 234: -1.74 ± 0.37 and Pro 236: -1.36 ± 0.30—all average energies are in kcal/mol denoted with the standard deviation.

Using the calculated energy contributions, two models have been derived in order to fit the experimental free binding energy. The first model (see Table III) used the following equation to predict the binding energy: $\Delta G_{model\ 1} = 0.24\ ELE + 0.28\ LJ - 0.57\ SA + 0.49\ PB + 0.023\ T\Delta S$ with a correlation coefficient r^2 of 0.865 and predictive ability, q^2, of 0.673. The standard error is 0.343 kcal/mol. In order to evaluate the predictive value of this method, a second model with compounds C, I and M in the test set was produced. The regression of the ten remaining compounds resulted in this equation: $\Delta G_{model\ 2} = 0.26\ ELE + 0.33\ LJ - 0.95SA + 0.53\ PB - 0.017\ T\Delta S$. This model shows r^2 of 0.814

Table III. Average electrostatic (ELE), hydrophobic (LJ), surface area (SA), Poisson-Boltzmann (PB) and entropic (TΔS) energy contributions to the free binding energy are given for all 13 compounds. Two models are shown using the energy contributions as descriptors. The first model is derived from a regression using all compounds. In the second model, compounds C, I and M were treated as a test set and were not included in the regression analysis.

Cmpd.	ELE	LJ	SA	PB	−TΔS	Model 1	Model 2
A	−17.67	−40.94	−4.33	2.781	12.67	−12.11	−12.284
B	−14.24	−40.09	−3.98	3.547	14.29	−10.917	−11.017
C	−17.81	−40.31	−4.06	3.219	11.29	−11.879	−12.161
D	−14.26	−45.74	−4.46	6.397	21.37	−10.998	−10.795
E	−13.12	−41.03	−4.49	2.402	15.84	−11.214	−11.138
F	−17.03	−41.36	−4.04	3.197	15.6	−12.104	−12.26
G	−13.28	−40.88	−4.12	4.111	12.83	−10.519	−10.622
H	−11.65	−48.39	−4.48	8.103	15.04	−10.124	−10.181
I	−15.86	−44.76	−4.37	4.371	26.41	−12.259	−11.956
J	−16.39	−41.03	−3.81	3.603	21.58	−11.931	−11.887
K	−16.07	−45.98	−4.09	3.64	17.02	−12.947	−13.23
L	−21.58	−41.27	−4.37	7.318	14.8	−10.959	−10.915
M	−23.41	−44.31	−4.11	9.503	17.02	−11.381	−11.438

and q^2 of 0.465. The decrease of q^2 can be explained by the drop in compounds used for the regression analysis. The calculated average error for the correlated compounds is 0.375 kcal/mol. With the obtained equation the energies of the test set were calculated. The differences to the experimental ΔG values were 0.584, −0.397 and 0.325 for compounds C, I and M, respectively. Regarding the error in the measurements of experimental values these residuals were still in an acceptable range.

In both models, the electrostatic and the Lennard–Jones energies were almost equally weighted. They are both of high significance with P-values below 0.001. It is not surprising that the hydrophobic interactions are the most substantial in this lipophilic binding pocket. The surface term is very small for all compounds and the differences between the inhibitors nearly negligible. The regression did not increase the importance of this energy contribution. In the regression analysis it proved to be not of high significance, which is represented in a P-value of 0.2. The Poisson–Boltzmann desolvation energy is again a contribution with high significance to the correlation with the experimental binding energy. The P-values are below 0.001 for both models. Characteristics beneficial for additional hydrogen bonding, akin to the ones found in compound M, also provide the compound with difficulties in desolvation, which is represented with this energy contribution. Since only a small part of the obtained trajectory snapshots were subject to this procedure the uncertainty is relatively high, namely 2.55 kcal/mol. And this term is highly dependent on the position of the ligand in each snapshot. The calculation of the entropy was again relatively uncertain with an average error of 7 kcal/mol. During the regression analysis this contribution was nearly removed and it showed the smallest significance of all contributions (P-value 0.4). Overall the regression performed remarkably well, most likely due to cancellation of errors. The correlation of both models to the experimental binding energy is shown in Figure 5.

Conclusion

In this work the interaction of the HIV-1 reverse transcriptase to a set of Efavirenz derivatives has been investigated using molecular dynamics simulations. Important interactions have been pointed out with regard to single residue contributions. In addition, this powerful method has been applied to provide a prediction of the binding free energy with the help of an established statistical method. The successful application of MD and subsequent calculations show that the proposed method is extremely potent and could provide genuine results even with a small set of

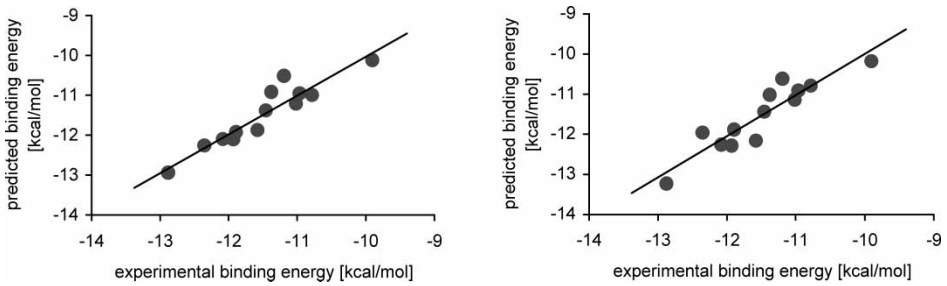

Figure 5. Correlation of the experimental and predicted binding energies of model 1 (left) and model 2 (right). The later includes the test set.

inhibitors. The fact that even small structural differences in the used ligand molecules resulted in good measurable differences further proves the value of MD as an investigative tool. In addition it was possible to incorporate a steric encumbranced compound into this study (compound H), which would meet with difficulties using methods that cannot take the high flexibility of the binding pocket into account. Without resorting to outliers a model of the binding energy was established with a correlation coefficient r^2 of 0.865 and predictive ability, q^2, of 0.673. Although this procedure is rather time consuming, the good result make this investment rewarding. Beside the prediction of the binding energy, chemically relevant energy contributions have been calculated which are descriptive by themselves. For example, resistance-mediating mutations are found for residues with large contributions to the binding energy.

Acknowledgements

The helpful discussions with Dr Anton Beyer are gratefully acknowledged. This investigation was supported by the Thailand Research Fund (BRG4780007) and the National Research Council of Thailand under Thai–Austria collaboration (1.AU 49/2547).

References

[1] Tantillo C, Ding JP, Jacobomolina A, Nanni RG, Boyer PL, Hughes SH, Pauwels R, Andries K, Janssen PAJ, Arnold E. J Mol Biol 1994;243:369–387.
[2] Young SD, Britcher SF, Tran LO, Payne LS, Lumma WC, Lyle TA, Huff JR, Anderson PS, Olsen DB, Carroll SS. Antimicrob Agents Chemother 1995;39:2602–2605.
[3] Bacheler LT, Anton ED, Kudish P, Baker D, Bunville J, Krakowski K, Bolling L, Aujay M, Wang XV, Ellis D, Becker MF, Lasut AL, George HJ, Spalding DR, Hollis G, Abremski K. Antimicrob Agents Chemother 2000;44:2475–2484.
[4] Shafer RW. Clin Microbiol Rev 2002;15:247–277.
[5] Ren J, Esnouf R, Garman E, Somers D, Ross C, Kirby I, Keeling J, Darby G, Jones Y, Stuart D, Stammers D. Nat Struct Biol 1995;2:293–302.
[6] Madrid M, Lukin JA, Madura JD, Ding J, Arnold E. Proteins 2001;45:176–182.
[7] Kensch O, Restle T, Woehrl BM, Goody RS, Steinhoff HJ. J Mol Biol 2000;301:1029–1039.
[8] Madrid M, Jacobo-Molina A, Ding J, Arnold E. Proteins 1999;35:332–337.
[9] Rizzo RC, Udier-Blagovic M, Wang D, Watkins EK, Kroeger Smith MB, Smith RH, Tirado-Rives J, Jorgensen WL. J Med Chem 2002;45:2970–2987.
[10] Udier-Blagovic M, Tirado-Rives J, Jorgensen WL. J Med Chem 2004;47:2389–2392.
[11] Gao J, Kuczera K, Tidor B, Karplus M. Science 1989;244:1069–1072.
[12] Ren J, Milton J, Weaver KL, Short SA, Stuart DI, Stammers DK. Struct Fold Des 2000;8:1089–1094.
[13] Patel M, Ko SS, McHugh Jr., RJ, Markwalder JA, Srivastava AS, Cordova BC, Klabe RM, Erickson- Viitanen S, Trainor GL, Seitz SP. Bioorg Med Chem Lett 1999;9:2805–2810.
[14] Patel M, McHugh Jr., RJ, Cordova BC, Klabe RM, Erickson-Viitanen S, Trainor GL, Ko SS. Bioorg Med Chem Lett 1999;9:3221–3224.
[15] Cornell WD, Cieplak P, Bayly CI, Kollman PA. J Am Chem Soc 1993;115:9620–9631.
[16] Cornell WD, Cieplak P, Bayly CI, Gould IR, Merz KM, Ferguson DM, Spellmeyer DC, Fox T, Caldwell JW, Kollman PA. J Am Chem Soc 1995;117:5179–5197.
[17] Frisch MJ, Trucks GW, Schlegel HB, Scuseria GE, Robb MA, Cheeseman JR, Montgomery Jr., JA, Vreven T, Kudin KN, Burant JC, Millam JM, Iyengar SS, Tomasi J, Barone V, Mennucci B, Cossi M, Scalmani G, Rega N, Petersson GA, Nakatsuji H, Hada M, Ehara M, Toyota K, Fukuda R, Hasegawa J, Ishida M, Nakajima T, Honda Y, Kitao O, Nakai H, Klene M, Li X, Knox JE, Hratchian HP, Cross JB, Adamo C, Jaramillo J, Gomperts R, Stratmann RE, Yazyev O, Austin AJ, Cammi R, Pomelli C, Ochterski JW, Ayala PY, Morokuma K, Voth GA, Salvador P, Dannenberg JJ, Zakrzewski VG, Dapprich S, Daniels AD, Strain MC, Farkas O, Malick DK, Rabuck AD, Raghavachari K, Foresman JB, Ortiz JV, Cui Q, Baboul AG, Clifford S, Cioslowski J, Stefanov BB, Liu G, Liashenko A, Piskorz P, Komaromi I, Martin RL, Fox DJ, Keith T, Al-Laham MA, Peng CY, Nanayakkara A, Challacombe M, Gill PMW, Johnson B, Chen W, Wong MW, Gonzalez C, Pople JA. Gaussian, Inc. 2003; Pittsburgh PA.
[18] Rarey M, Kramer B, Lengauer T, Klebe G. J Mol Biol 1996;261:470–489.
[19] Pearlman DA, Case DA, Caldwell JW, Ross WR, Cheatham TE, DeBolt S, Ferguson D, Seibel G, Kollman P. Comp Phys Commun 1995;91:1–41.
[20] Berendsen HJC, Postma JPM, van Gunsteren WF, DiNola A, Haak JR. J Chem Phys 1984;81:3684–3690.
[21] Wang J, Morin P, Wang W, Kollman PA. J Am Chem Soc 2001;123:5221–5230.
[22] Chong LT, Duan Y, Wang L, Massova I, Kollman PA. Proc Natl Acad Soc 1999;96:14330–14335.
[23] Srinivansan J, Miller J, Kollman PA, Case DA. J Biol Struct Dyn 1998;16:671–682.
[24] Connolly ML. Analytical molecular surface calculation. J Appl Cryst 1983;16:548–558.
[25] Baker NA, Sept D, Joseph S, Holst MJ, McCammon JA. Proc Natl Acad Sci USA 2001;98:10037–10041.
[26] Hsiou Y, Ding J, Das K, Clark Jr., AD, Boyer PL, Lewi P, Janssen PAJ, Kleim JP, Roesner M, Hughes SH, Arnold E. J Mol Biol 2001;309:437–445.
[27] Åqvist J, Medina C, Samuelsson J-E. Protein Eng 1994;7:385–391.
[28] Carlson HA, Jorgensen WL. J Phys Chem 1995;99: 10667–10673.
[29] Romero DL, Olmsted RA, Poel TJ, Morge RA, Biles C, Keiser BJ, Kopta LA, Friis JM, Hosley JD, Stefanski KJ, Wishka DG, Evans DB, Morris J, Stehle RG, Sharma SK, Yagi Y, Voorman RL, Adams WJ, Tarpley WG. J Med Chem 1996;39:3769–3789.